Scientia Iranica F (2014) 21(3), 1197–1207

Sharif University of Technology
Scientia Iranica
Transactions F: Nanotechnology
www.scientiairanica.com

Research Note

Frequency response of skew and trapezoidal shaped mono-layer graphene sheets via discrete singular convolution

B. Akgöz and Ö. Civalek*

Division of Mechanics, Department of Civil Engineering, Faculty of Engineering, Akdeniz University, Antalya, Turkey.

Received 23 May 2013; received in revised form 20 February 2014; accepted 8 April 2014

KEYWORDS
Graphene sheet;
Frequency;
Discrete singular convolution;
Skew shaped graphene;
Vibration.

Abstract. In the present study, the frequency response of skew and trapezoidal shaped single layer graphene sheets are studied via Kirchhoff plate theory. A four node Discrete Singular Convolution (DSC) method is developed for free vibration analysis of arbitrary straight-sided quadrilateral graphene. The straight-sided skew and trapezoidal graphene is mapped into a square graphene in the computational space using a four-node element. By using the geometric transformation, the governing equations and boundary conditions of the graphene are transformed from the physical domain into a square computational domain. Numerical examples illustrating the accuracy and convergence of the DSC method for skew and trapezoidal shaped graphene sheets are presented. New results for skew and trapezoidal shaped graphene have been presented, which can serve as benchmark solutions for future investigations.

1. Introduction

Nanomechanics are a popular branch of nano-sciences. The aim of this new area is to define some of the fundamental physical properties of nano-scaled structures. In general, atomistic modeling and continuum modeling are adopted foe modeling of the mechanical properties of these nano-scaled systems. Carbon nanotubes (CNTs) and Graphene Sheets (GS) are two-novel forms of carbon [1-4]. Due to their superior physical, electrical and chemical properties, both carbon nanotubes and the graphene sheets have been widely used in many disciplines, such as Nano-Electro-Mechanical Systems (NEMS), biomechanics, computers, and medical and optic applications [5-9].

Straight-sided quadrilateral graphenes are used in modern engineering applications, such as nano-electro-mechanical components. Knowledge of the free vibration characteristics of these structures is very important during the design process. The vibration analysis of carbon nanotubes and graphene may be either analytical or numerical [10-15]. It is well known that the experimental or atomic based solutions of such problems can be obtained for only certain simple cases of rectangular and square shapes. Consequently, employment of classical or higher-order continuum approaches is an efficient alternative [16-26]. The analysis of non-rectangular graphenes or, as generally called, straight-sided quadrilateral graphenes, has been a research subject in nanomechanics and modern industries. In the past, geometric transformation was used for non-rectangular plate analysis [27,28]. However, in the past fifty years, finite element methods have been widely used in mathematical physics and engineering. Solutions of initial and boundary value problems have always been issues of interest to engineering and phys-

*. *Corresponding author. Tel.: + 90- 242-310 6319; Fax: +90-242-310 6306*
E-mail address: civalek@yahoo.com (Ö. Civalek)

ical sciences, and many different numerical approaches have been used for computational purposes. In this regard, in general, finite difference, finite element, Ritz, and boundary element methods have become very popular, and these numerical approaches are used extensively for solving engineering problems. The method of Discrete Singular Convolution (DSC) is a relatively new numerical technique for the numerical solution of partial and ordinary differential equations. DSC is a novel type of numerical approach for approximate numerical solutions of differential equations proposed by Wei [29]. In the literature, Wei and his co-workers firstly applied the DSC algorithm to solve some mathematical physics problems [30-35]. Zhao et al. [36-38] analyzed the high frequency vibration of plates using the DSC algorithm, and Hou et al. [39] investigated the DSC based Ritz approach for the dynamic analysis of thin and thick plates. These studies indicate that the DSC algorithm works very well for the modeling and solution of mechanical problems [40,41]. It is also concluded that the discrete singular convolution technique has a global method accuracy and a local method flexibility for solving ordinary and partial differential equations in physics and engineering problems [42-50]. Numerical solution of the free vibration problem of plates and shells has also been investigated by the present author [51-57]. Wei states that the mathematical base of the singular convolution technique is the theory of distributions and some types of wavelet analysis. [29-31]. The primary objective of this study is to give a numerical solution of the free vibration analysis of straight-sided quadrilateral graphene sheets. Using a four-node element, the straight-sided quadrilateral domain is mapped into a square domain in computational space. To the author's knowledge, it is the first time that free vibration has been successfully obtained for skew and trapezoidal graphene sheets. Furthermore, new results for the frequency values of skew and trapezoidal shaped graphene have been presented, which can serve as benchmark solutions for future investigations.

2. Discrete Singular Convolution (DSC)

Using the same notations and similar parameters, let us consider a distribution, T and $\eta(t)$, as an element of the space of the test or trial function. Thus, we can define the typical singular convolution as [29]:

$$F(t) = (T * \eta)(t) = \int_{-\infty}^{\infty} T(t-x)\eta(x)dx. \tag{1}$$

The operator $T(t-x)$ is known as a singular kernel. Many types of kernel have been used in the literature. For example, singular kernels of a delta type [30] is:

$$T(x) = \delta^{(n)}(x); \quad (n = 0, 1, 2, ...,). \tag{2}$$

The kernel given in Eq. (2), $T(x) = \delta(x)$, is important for interpolation of surfaces and curves, and $T(x) = \delta^{(n)}(x)$ for $n > 1$ are requisite for numerical solution of differential equations. It is also known that the following form is more effective for discrete singular convolution with a sufficiently smooth approximation [31]:

$$F_a(t) = \sum_k T_a(t - x_k) f(x_k), \tag{3}$$

where $F_a(t)$ is an approximation of $F(t)$, and $\{x_k\}$ is an appropriate set of discrete points on which the discrete singular convolution in Eq. (3) is well defined. It must also be defined that the original test function, $\eta(x)$, has been replaced by $f(x)$ for computer realization purpose [31,32]. After some successful applications in mathematical physics and applied mechanics, the use of some type of kernel and regularizer, such as a delta regularizer, was proposed [32-37]. For example, a well-known kernel is the Shannon kernel, and it is regularized as the following relation [38]:

$$\delta_{\Delta,\sigma}(x - x_k) = \frac{\sin[(\pi/\Delta)(x - x_k)]}{(\pi/\Delta)(x - x_k)} \exp \times \left[-\frac{(x - x_k)^2}{2\sigma^2} \right]; \quad \sigma > 0. \tag{4}$$

Eq. (4) can also be used to provide discrete approximations of the singular convolution kernels of the delta type [40]:

$$f^{(n)}(x) \approx \sum_{k=-M}^{M} \delta_\Delta(x - x_k) f(x_k), \tag{5}$$

where $\delta_\Delta(x - x_k) = \Delta\delta_a(x - x_k)$ and superscript (n) denotes the nth-order derivative, and $2M + 1$ is the computational bandwidth, which is centered around x and is usually smaller than the whole computational domain. For example, the Dirichlet kernel has one more M parameter for computation. In the DSC method, function $f(x)$ and its derivatives, with respect to the x coordinate at a grid point x_i, are approximated by a linear sum of discrete values of function $f(x_k)$ in a narrow bandwidth $[x - x_M, x + x_M]$, namely [41]:

$$\left.\frac{d^n f(x)}{dx^n}\right|_{x-x_i} = f^{(n)}(x) \approx \sum_{k=-M}^{M} \delta_{\Delta,\sigma}^{(n)}(x_i - x_k) f(x_k); \quad (n = 0, 1, 2, ...,), \tag{6}$$

where superscript n denotes the nth-order derivative with respect to x. The x_k is a set of discrete sampling points centered around point x, σ is a regularization parameter, Δ is the grid spacing, and $2M + 1$ is the computational bandwidth, which is usually smaller than the size of the computational domain. For example, the second order derivative at $x = x_i$ of the DSC kernels are directly given in discretized form as [41]:

$$f^{(2)}(x) = \left.\frac{d^2 f}{dx^2}\right|_{x=x_i} \approx \sum_{k=-M}^{M} \delta^{(2)}_{\Delta,\sigma}(k\Delta x_N) f_{i+k,j}. \quad (7)$$

In the above equation, $M + 1$ is the effective kernel support. In these equations, the related derivatives can be listed in the literature [35-41]. The fourth-order derivative is defined as follows [42,43]:

$$\begin{aligned}
\delta^{(4)}_{\pi/\Delta,\sigma}(x_m - x_k) &= 4\frac{(\pi^2/\Delta^2)\cos(\pi/\Delta)(x-x_k)}{(x-x_k)^2} \\
&\times\exp\left[\frac{-(x-x_k)^2}{2\sigma^2}\right] + \frac{(\pi^3/\Delta^3)\sin(\pi/\Delta)(x-x_k)}{(x-x_k)} \\
&\times\exp\left[\frac{-(x-x_k)^2}{2\sigma^2}\right] + 4\frac{(\pi^2/\Delta^2)\cos(\pi/\Delta)(x-x_k)}{\sigma^2} \\
&\times\exp\left[\frac{-(x-x_k)^2}{2\sigma^2}\right] - 12\frac{(\pi/\Delta)\sin(\pi/\Delta)(x-x_k)}{(x-x_k)^3} \\
&\times\exp\left[\frac{-(x-x_k)^2}{2\sigma^2}\right] - 6\frac{(\pi/\Delta)\sin(\pi/\Delta)(x-x_k)}{(x-x_k)\sigma^2} \\
&\times\exp\left[\frac{-(x-x_k)^2}{2\sigma^2}\right] - 6\frac{(\pi/\Delta)(x-x_k)\sin(\pi/\Delta)(x-x_k)}{\sigma^4} \\
&\times\exp\left[\frac{-(x-x_k)^2}{2\sigma^2}\right] - 24\frac{\cos(\pi/\Delta)(x-x_k)}{(x-x_k)^4} \\
&\times\exp\left[\frac{-(x-x_k)^2}{2\sigma^2}\right] - 12\frac{\cos(\pi/\Delta)(x-x_k)}{(x-x_k)^2\sigma^2} \\
&\times\exp\left[\frac{-(x-x_k)^2}{2\sigma^2}\right] - 4\frac{(x-x_k)^2\cos(\pi/\Delta)(x-x_k)}{\sigma^6} \\
&\times\exp\left[\frac{-(x-x_k)^2}{2\sigma^2}\right] + 24\frac{\sin(\pi/\Delta)(x-x_k)}{\pi(x-x_k)^5/\Delta} \\
&\times\exp\left[\frac{-(x-x_k)^2}{2\sigma^2}\right] + 12\frac{\sin(\pi/\Delta)(x-x_k)}{\pi\sigma^6(x-x_k)^3/\Delta} \\
&\times\exp\left[\frac{-(x-x_k)^2}{2\sigma^2}\right] + 3\frac{\sin(\pi/\Delta)(x-x_k)}{\pi(x-x_k)\sigma^4/\Delta} \\
&\times\exp\left[\frac{-(x-x_k)^2}{2\sigma^2}\right] - 2\frac{(x-x_k)\sin(\pi/\Delta)(x-x_k)}{(\pi\sigma^6/\Delta)} \\
&\times\exp\left[\frac{-(x-x_k)^2}{2\sigma^2}\right] + \frac{(x-x_k)^3\sin(\pi/\Delta)(x-x_k)}{\pi\sigma^8/\Delta} \\
&\times\exp\left[\frac{-(x-x_k)^2}{2\sigma^2}\right]. \qquad (8)
\end{aligned}$$

Discrete singular convolution has many potential applications for computer realization (e.g. Hilbert, Radon, Delta and Abel transforms).

3. Domain transformation for skew field

The method of DSC is not suitable for an irregular domain. Consider an arbitrary (straight-sided), quadrilateral, mono-layer graphene sheet, as shown in Figure 1. The geometry of this graphene can be mapped into a rectangular graphene in the natural $\xi - \eta$ plane, as shown in this figure. By employing the following four-node transformation equations, the physical domain is mapped into the computational domain [27]:

$$x = \sum_{i-1}^{N} x_i \Lambda_i(\xi,\eta), \quad (9a)$$

$$y = \sum_{i=1}^{N} y_i \Lambda_i(\xi,\eta), \quad (9b)$$

where x_i and y_i are the coordinates of node i in the physical domain, N is the number of grid points, and $\Lambda_i(\xi,\eta)$, $i = 1, 2, 3, ..., N$, are the interpolation (shape) functions. These are given for node i [28,29]:

$$\Lambda_i(\xi,\eta) = \frac{1}{4}(1+\xi\xi_i)(1+\eta\eta_i). \quad (10)$$

Thus, the first-order and second order derivatives of function g are defined as [27]:

$$\begin{Bmatrix} g_x \\ g_y \end{Bmatrix} = [H_{11}]^{-1}\begin{Bmatrix} g_\xi \\ g_\eta \end{Bmatrix}, \quad (11)$$

$$\begin{Bmatrix} g_{xx} \\ g_{yy} \\ 2g_{yx} \end{Bmatrix} = [H_{22}]^{-1}\begin{Bmatrix} g_{\xi\xi} \\ g_{\eta\eta} \\ 2g_{\xi\eta} \end{Bmatrix} - [H_{22}]^{-1}[H_{21}][H_{11}]^{-1}\begin{Bmatrix} g_\xi \\ g_\eta \end{Bmatrix}, \quad (12)$$

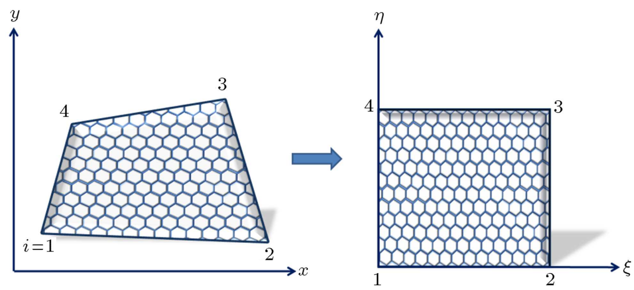

Figure 1. Mapping of arbitrary quadrilateral plates into natural coordinates.

where ξ_i and η_i are the coordinates of node i in the $\xi - \eta$ plane, and H_{ij} are the elements of the Jacobian matrix. These are expressed as follows [27]:

$$[H_{11}] = \begin{bmatrix} x_\xi & y_\xi \\ x_\eta & y_\eta \end{bmatrix}, \quad [H_{21}] = \begin{bmatrix} x_{\xi\xi} & y_{\xi\xi} \\ x_{\eta\eta} & y_{\eta\eta} \\ x_{\xi\eta} & y_{\xi\eta} \end{bmatrix}, \tag{13}$$

$$[H_{22}] = \begin{bmatrix} x_\xi^2 & y_\xi^2 & x_\xi y_\xi \\ x_\eta^2 & y_\eta^2 & x_\eta y_\eta \\ x_\xi x_\eta & y_\xi y_\eta & \frac{1}{2}(x_\xi y_\eta + x_\eta y_\xi) \end{bmatrix}. \tag{14}$$

Consequently, an arbitrary-shaped quadrilateral graphene may be represented by the mapping of a square graphene defined in terms of its natural coordinates. Using the above procedure, the second-order derivatives, with respect to the $-x$ coordinate, can be written as:

$$\frac{\partial^2 w}{\partial x^2} = [H_{22}]^{-1} \sum_{i=-M}^{M} \delta_{\Delta,\sigma}^{(2)}(k\Delta\xi) w_{ik} - [H_{22}]^{-1}[H_{21}][H_{11}]^{-1} \sum_{i=-M}^{M} \delta_{\Delta,\sigma}^{(1)}(k\Delta\xi) w_{ik}, \tag{15}$$

$$\frac{\partial^2 w}{\partial x^2} = [H_{11}]^{-1} \sum_{i=-M}^{M} \delta_{\Delta,\sigma}^{(1)}(k\Delta\xi) w_{ik}. \tag{16}$$

4. Governing equations

Graphene sheet is very strong and has high rigidity. An atomistic model is expensive and needs large computer capacity. Experimental studies can be undertaken for only some specific cases. So, the modeling of graphene sheets as a continuum plate model is generally used by researchers. For non-rectangular grapheme, some important studies can be found in literature [59,60]. The nonlocal continuum plate model is used for the modeling of quadrilateral graphene sheets by Babaei and Shahidi [59], and the free vibration analysis of orthotropic non-prismatic skew nanoplates is presented by Alibeygi Beni and Malekzadeh [60].

The governing equation of a single layer graphene in vibration is written as:

$$D\left(\frac{\partial^4 w}{\partial x^4} + 2\frac{\partial^4 w}{\partial x^2 \partial y^2} + \frac{\partial^4 w}{\partial y^4}\right) - \rho h \frac{\partial^2 w}{\partial t^2} = 0, \tag{17}$$

where D is the coefficient of the bending rigidity for graphene, h is the thickness, w is the deflection, ρ is the density, and x and y are the midplane Cartesian coordinates. The transverse displacement, w, for free vibration is taken as:

$$w(x,y,t) = W(x,y)e^{iwt}. \tag{18}$$

Substituting Eq. (18) into Eq. (17), one obtains the normalized equation:

$$\frac{\partial^4 W}{\partial X^4} + 2\lambda^2 \frac{\partial^4 W}{\partial X^2 \partial Y^2} + \lambda^4 \frac{\partial^4 W}{\partial Y^4} = \Omega^2 W. \tag{19}$$

The non-dimensional quantities are:

$$X = x/a, \quad Y = y/b,$$

$$\lambda = a/b, \quad \Omega^2 = \rho h a^4 \omega^2 / D. \tag{20}$$

Eq. (19) takes the following simple form:

$$\nabla^2 \nabla^2 (W_{XY}) = \Omega^2 W, \tag{21}$$

where ∇^2 is the Laplace operator. Consider the following differential operators before discretizing the governing differential equations:

$$F = \frac{\partial^2 W}{\partial X^2}, \tag{22}$$

$$G = \frac{\partial^2 W}{\partial Y^2}. \tag{23}$$

Thus, the fourth-order derivatives can be given in terms of the second order derivatives, that is:

$$\frac{\partial^4 W}{\partial X^4} = \frac{\partial^2}{\partial X^2} F, \tag{24}$$

$$\frac{\partial^4 W}{\partial Y^4} = \frac{\partial^2}{\partial Y^2} G, \tag{25}$$

$$\frac{\partial^4 W}{\partial X^2 \partial Y^2} = \frac{\partial^2}{\partial X^2}\left[\frac{\partial^2 w}{\partial Y^2}\right] = \frac{\partial^2}{\partial X^2} G. \tag{26}$$

After using the geometric transformation process, the following form can be given for the first, second, and fourth-order derivatives:

$$\frac{\partial W}{\partial X} = [H_{11}]^{-1} \frac{\partial W}{\partial \xi}, \tag{27a}$$

$$\frac{\partial W}{\partial Y} = [H_{11}]^{-1} \frac{\partial W}{\partial \eta}, \tag{27b}$$

$$\frac{\partial^2 W}{\partial X^2} = [H_{22}]^{-1} \frac{\partial^2 W}{\partial \xi^2} - [H_{22}]^{-1}[H_{21}][H_{11}]^{-1} \frac{\partial W}{\partial \xi}, \tag{27c}$$

$$\frac{\partial^2 W}{\partial Y^2} = [H_{22}]^{-1} \frac{\partial^2 W}{\partial \eta^2} - [H_{22}]^{-1}[H_{21}][H_{11}]^{-1} \frac{\partial W}{\partial \eta}, \tag{27d}$$

and:

$$\frac{\partial^4 W}{\partial X^4} = \frac{\partial^2 F}{\partial \xi^2} = [H_{22}]^{-1} \frac{\partial^2 F}{\partial \xi^2} - [H_{22}]^{-1}[H_{21}][H_{11}]^{-1} \frac{\partial F}{\partial \xi}, \tag{28a}$$

$$\frac{\partial^4 W}{\partial Y^4} = \frac{\partial^2 G}{\partial \eta^2} = [H_{22}]^{-1}\frac{\partial^2 G}{\partial \eta^2} - [H_{22}]^{-1}[H_{21}][H_{11}]^{-1}\frac{\partial G}{\partial \eta}, \quad (28b)$$

$$\frac{\partial^4 W}{\partial X^2 \partial Y^2} = \frac{\partial^2 G}{\partial X^2} = [H_{22}]^{-1}\frac{\partial^2 S}{\partial \xi^2} - [H_{22}]^{-1}[H_{21}][H_{11}]^{-1}\frac{\partial S}{\partial \xi}. \quad (28c)$$

Using the differential operators in Eqs. (27) and (28); the normalized governing equation, i.e. Eq. (21), takes the following form:

$$\frac{\partial^2 F}{\partial X^2} + 2\lambda^2\frac{\partial^2 G}{\partial X^2} + \lambda^4\frac{\partial^2 G}{\partial Y^2} = \Omega^2 W, \quad (29)$$

or:

$$\nabla^2(W_{\xi\eta}) = \Omega^2 W. \quad (30)$$

Employing the transformation rule, governing Eq. (30) becomes:

$$[H_{22}]^{-1}\frac{\partial^2 F}{\partial \xi^2} - [H_{22}]^{-1}[H_{21}][H_{11}]^{-1}\frac{\partial F}{\partial \xi} + 2\lambda^2\left([H_{22}]^{-1}\frac{\partial^2 F}{\partial \eta^2} - [H_{22}]^{-1}[H_{21}][H_{11}]^{-1}\frac{\partial F}{\partial \eta}\right) + \lambda^4\left([H_{22}]^{-1}\frac{\partial^2 G}{\partial \eta^2} - [H_{22}]^{-1}[H_{21}][H_{11}]^{-1}\frac{\partial G}{\partial \eta}\right) = \Omega^2 W. \quad (31)$$

Substituting the discrete singular convolution procedure from Eq. (6) into Eq. (31), one can obtain the discrete analog of the governing equations as:

$$[H_{22}]^{-1}\left[\sum_{k=-M}^{M}\delta^{(2)}_{\Delta,\sigma}(k\Delta\xi)F_{kj} + 2\lambda^2\sum_{k=-M}^{M}\delta^{(2)}_{\Delta,\sigma}(k\Delta\eta)F_{ik} + \lambda^4\sum_{k=-M}^{M}\delta^{(2)}_{\Delta,\sigma}(k\Delta\eta)G_{ik}\right] - [H_{22}]^{-1}[H_{21}][H_{11}]^{-1}\left(\sum_{k=-M}^{M}\delta^{(1)}_{\Delta,\sigma}(k\Delta\xi)F_{kj} + 2\lambda^2\sum_{k=-M}^{M}\delta^{(1)}_{\Delta,\sigma}(k\Delta\eta)F_{ik} + \lambda^4\sum_{k=-M}^{M}\delta^{(1)}_{\Delta,\sigma}(k\Delta\eta)G_{ik}\right) = \Omega^2 W_{ij}. \quad (32)$$

At this stage, the following new variable is introduced for simplicity:

$$\Im = (k\Delta\xi)F_{kj} + 2\lambda^2(k\Delta\xi)F_{ik} + \lambda^4(k\Delta\eta)G_{ik}. \quad (33)$$

Using this new operator, the governing equations of a plate for free vibration can be expressed as:

$$[H_{22}]^{-1}\left[\sum_{k=-M}^{M}\delta^{(2)}_{\Delta,\sigma}\Im\right] - [H_{22}]^{-1}[H_{21}][H_{11}]^{-1} \times \left[\sum_{k=-M}^{M}\delta^{(1)}_{\Delta,\sigma}\Im\right] = \Omega^2 W_{ij}. \quad (34)$$

To obtain the discretized form of Eq. (32) in its natural coordinate, we apply Eq. (34) to the following equation:

$$\nabla^4(W_{\xi\eta}) = \nabla^2\nabla^2(W_{\xi\eta}) = \Omega^2 W. \quad (35)$$

Substituting Eq. (34) into Eq. (35), the governing equation can now be obtained as:

$$\left([H_{22}]^{-1}\left[\sum_{k=-M}^{M}\delta^{(2)}_{\Delta,\sigma}\Im\right] - [H_{22}]^{-1}[H_{21}][H_{11}]^{-1} \times \left[\sum_{k=-M}^{M}\delta^{(1)}_{\Delta,\sigma}\Im\right] \times [H_{22}]^{-1}\left[\sum_{k=-M}^{M}\delta^{(2)}_{\Delta,\sigma}\Im\right] - [H_{22}]^{-1}[H_{21}][H_{11}]^{-1}\left[\sum_{k=-M}^{M}\delta^{(1)}_{\Delta,\sigma}\Im\right]\right) = \Omega^2 W_{ij}. \quad (36)$$

Therefore, the governing equation is given by the matrix notation as:

$$(\mathbf{D}^4_\xi \otimes \mathbf{I}_\eta + 2\lambda^2\mathbf{D}^2_\xi \otimes \mathbf{D}^2_\eta + \lambda^4\mathbf{I}_\xi \otimes \mathbf{D}^4_\eta)\mathbf{W} = \mathbf{\Omega^2 W}, \quad (37)$$

where $\mathbf{I}_\xi$ and $\mathbf{I}_\eta$ are the $(N_r+1)^2$; $(r=\xi,\eta)$ unit matrix and $\otimes$ is used as the manner of tensorial product. In this study, two types of boundary condition (simply supported and clamped) are taken into consideration for graphene sheet. The related formulations and their DSC form [33-41] are given in detail in the following:

Simply supported edge (S):

$$W = 0, \quad -D\left(\frac{\partial^2 W}{\partial n^2} + v\frac{\partial^2 W}{\partial S^2}\right) = 0. \quad (38)$$

Clamped edge (C):

$$W = 0, \quad \frac{\partial W}{\partial n} = 0, \quad (39)$$

where n and s denote the normal and tangential directions of the plate, respectively. The discrete form of the related boundary conditions can be given as follows [36,37,52,53]:

Simply supported edge (S):

$$W_{ij}=0, \tag{40}$$

$$-\left(\delta^{(2)}_{\sigma,\Delta}(X_i-X_0)+\sum_{j=0}^{J}(1-a_i)\delta^{(2)}_{\sigma,\Delta}(X_i-X_j)\right)W(X_0)$$

$$+\sum_{j=0}^{J}(1+a_i)\delta^{(2)}_{\sigma,\Delta}(X_i-X_j)W(X_i)$$

$$+v\left\{\left(\delta^{(2)}_{\sigma,\Delta}(Y_i-Y_0)+\sum_{j=0}^{J}(1-a_i)\delta^{(2)}_{\sigma,\Delta}(Y_i-Y_j)\right)\right.$$

$$\left.\times W(Y_0)+\sum_{j=0}^{J}(1+a_i)\delta^{(2)}_{\sigma,\Delta}(Y_i-Y_j)W(Y_i)\right\}=0. \tag{41}$$

Clamped edge (C):

$$W_{ij}=0, \tag{42}$$

$$\left(\delta^{(1)}_{\sigma,\Delta}(X_i-X_{N-1})-\sum_{j=0}^{J}(1-a_i)\delta^{(1)}_{\sigma,\Delta}(X_i-X_j)\right)$$

$$\times W(X_{N-1})+\sum_{j=0}^{J}(1-a_i)\delta^{(1)}_{\sigma,\delta}(X_i-X_j)\times W(X_i). \tag{43}$$

After implementation of the boundary conditions, Eq. (37) is rewritten as:

$$(\mathbf{D}^{*4}_{\xi}\otimes\mathbf{I}_{\eta}+2\lambda^2\mathbf{D}^{*2}_{\xi}\otimes\mathbf{D}^{*2}_{\eta}+\lambda^4\mathbf{I}_{\xi}\otimes\mathbf{D}^{*4}_{\eta})W=\Omega^2W. \tag{44}$$

Here, $\mathbf{D}^{*n}_{r}$ is $(N-2)\times(N-2)$.

5. Numerical results

The numerical solutions of the vibration response of skew and trapezoidal shaped graphene sheets are shown in Figure 2, under various geometric parameters and boundary conditions. In these analyses, the material properties of the graphene layer are taken as follows: $E=1$ TPa, $v=0.16$, $\rho=2250$ kg/m^3. The results given in this section are aimed to illustrate the numerical accuracy of the proposed DSC based coordinate transformation method. The graphenes of various planforms are designated by the boundary conditions at their edges.

For the verification of the proposed model, we simulate the vibration of a single layer square graphene sheet. The graphene has different lengths, from 10 nm to 40 nm. For comparison purposes, we use the value of 0.34 nm for the thickness of the graphene layer.

The Young's modulus is 1 TPa. In Table 1, the effects of different values of N on the convergence of the first five frequencies for SSSS skew graphene sheets of $a/b=1$, ($\alpha=75°$, $b=10$ nm) are presented. It is shown that the results are good for $N=13$ for first frequencies. For second and other higher modes of vibration, however, accurate results are obtained for $N=15$. Based on this convergence study, unless otherwise indicated, we set the grid number as $N=15$. Table 2 contains the fundamental frequencies (THz)

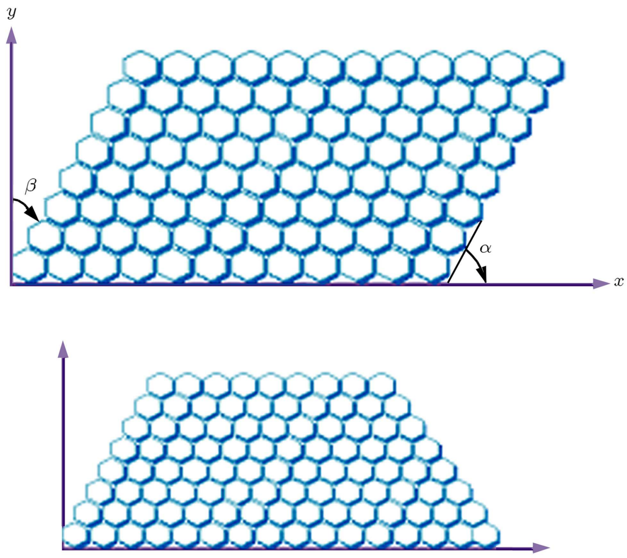

Figure 2. A typical skew and trapezoidal graphene.

Table 1. Frequency values (THz) of SSSS skew graphene sheets ($a/b=1$; $\alpha=75°$, $b=10$ nm).

Frequency mode	Present numerical results			
	$N=9$	$N=13$	$N=15$	$N=17$
1	0.07005	0.06951	0.06949	0.06949
2	0.17023	0.16094	0.16050	0.16050
3	0.19302	0.18703	0.18690	0.18691
4	0.28241	0.26386	0.26324	0.26323
5	0.35377	0.34685	0.34645	0.34642

Table 2. Fundamental frequency values (THz) of SSSS square graphene sheets ($a/b=1$, $\alpha=90°$, $N=15$).

a (nm)	Molecular dynamics (zigzag) [58]	Molecular dynamics (armchair) [58]	Present DSC
10	0.05877	0.05950	0.06503
20	0.01575	0.01581	0.01628
30	0.00706	0.00707	0.00716
40	0.00409	0.00410	0.00410

of SSSS square graphene. Four different length values are taken into consideration. The results are compared with those obtained by molecular dynamics (zigzag) and molecular dynamics (armchair) approaches by Ansari et al. [58]. The results are in good agreement compared with those presented by Ansari et al. [58] for the longest length value.

Some benchmark results are presented in Tables 3-6 for skew and trapezoidal shaped graphene sheets, respectively. The fundamental frequency parameters are given in Table 3 for skew graphenes, with skew angles varying from 30° to 75°. Three different boundary conditions are considered. It is shown that the increasing value of skew angle (as α) always decreases the frequency parameter for all types of boundary condition. In literature [59], the angle is taken between the axis-y and the skew side of the grapheme, as β in Figure 2. So, the frequency value

Table 3. Fundamental frequency values (THz) of skew graphene sheets ($a/b = 1$).

α	SSSS	CCCC	SCSC
75	0.06949	0.12717	0.10219
60	0.08311	0.15348	0.12307
45	0.11764	0.21865	0.17483
30	0.22078	0.40566	0.32391

Table 4. Frequency values (THz) of skew graphene sheets (CCCC) for different aspect ratio.

α	$b/a = 1$	$b/a = 2$	$b/a = 3$
45	0.21865	0.15773	0.15226
60	0.15363	0.10732	0.10226
90	0.11982	0.08187	0.07728

Table 5. Frequency values (THz) of SCSC trapezoidal graphene sheets ($a/b = 1$; $c/a = 0.2$).

Frequency mode	$N = 13$	$N = 15$	$N = 17$
1	0.15291	0.15283	0.15283
2	0.31024	0.31012	0.31012
3	0.36222	0.36220	0.36218
4	0.51881	0.51871	0.51877
5	0.60186	0.60179	0.60178
6	0.65342	0.65336	0.65334

Table 6. Frequency values (THz) of CCCC trapezoidal graphene sheets ($b/a = 1$).

Mode	$c/a = 0.2$	$c/a = 0.4$	$c/a = 0.7$
1	0.1258	0.1026	0.0773
2	0.2653	0.2131	0.1736
3	0.3304	0.2763	0.2108

increases with increasing the skew angles (β). In fact, our own conclusions and those in the literature are in agreement. The CCCC skew graphene has the highest frequency parameter, followed by SCSC and SSSS type boundary conditions. In other words, the effect of boundary conditions on the vibration behavior of graphene is significant. Fundamental frequencies (THz) of skew graphene sheets (CCCC) for different aspect ratios have been presented in Table 4. Depending on the increase in aspect ratio, b/a, the effect of the skew angle on the frequency becomes insignificant. Frequency values (THz) of trapezoidal graphene sheets are calculated and presented in Tables 5-6 for different geometric parameters. It is shown that the increasing value of c/a always decreases the frequency parameter. Frequency responses of skew shaped mono-layer SSSS graphene sheets for different skew angles ($a/b = 1$) are depicted in Figure 3 for different mode numbers. It is found from this figure that, as the skew angle is increased, the frequency values tend to decrease. However, the effect of skew angle on the frequency parameter is more significant for the higher modes. Namely, the frequency parameter decreases rapidly for small skew angle ratios and, then, gradually decreases with increasing skew angles.

The effect of aspect ratio on the frequency response of skew shaped mono-layer SSSS graphene sheets for different skew angles is depicted in Figure 4. Generally, it can be seen that, as b/a increases, with fixed skew angle, the frequencies decrease. Also, the effect of the skew angle on the frequency parameter is more significant for small aspect ratios.

The relationships between frequency parameter and mode number for skew graphene are depicted in Figure 5 for different skew angles. Variations of

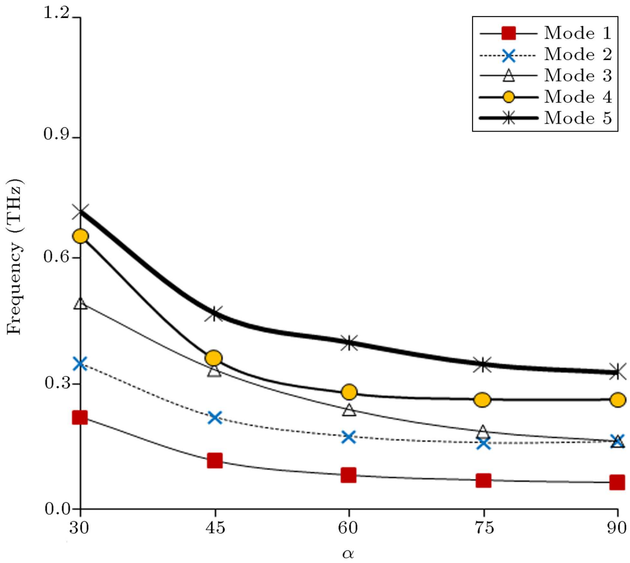

Figure 3. Frequency response of skew shaped mono-layer SSSS graphene sheets for different skew angles ($a/b = 1$).

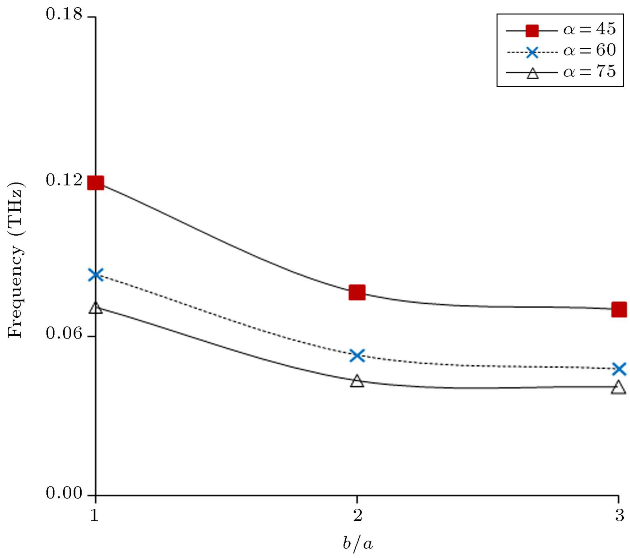

Figure 4. Frequency response of skew shaped mono-layer SSSS graphene sheets for different aspect ratio.

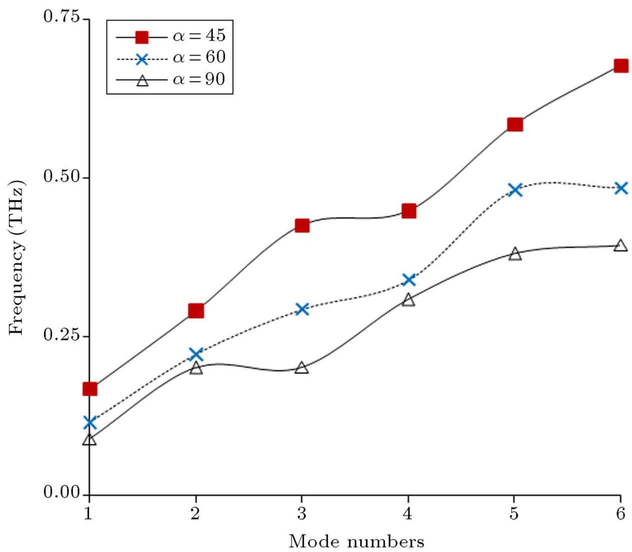

Figure 5. Frequencies of skew shaped mono-layer CCSS graphene sheets for different mode numbers.

the frequency parameter of skew shaped mono-layer graphene sheets, for different boundary conditions and mode number, is figured in Figure 6. From these two figures, it can be concluded that the increasing value of the mode number always increases the frequency parameter for all types of boundary condition and skew angle.

6. Concluding remarks

Skew and trapezoidal shaped graphene has found applications in the area of micro-computers and micro-medical applications. In the present paper, the frequency behavior of straight-sided quadrilateral graphene sheets is presented. Using the geometric

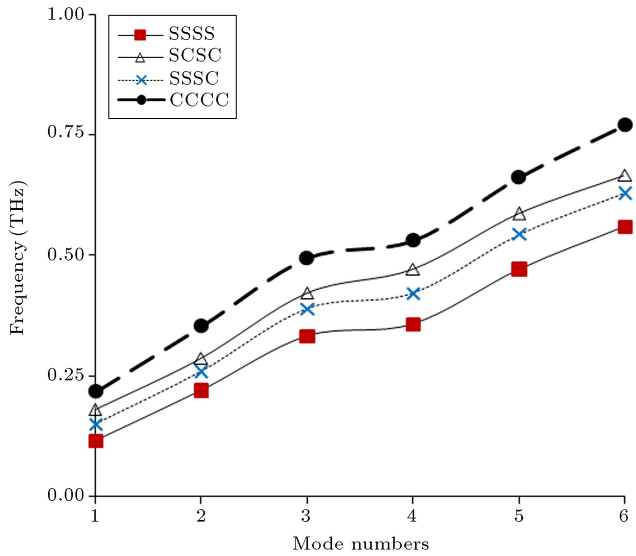

Figure 6. Frequencies of skew shaped mono-layer graphene sheets for different boundary conditions.

transformation, the governing equations and boundary conditions of the mono-layer graphene are transformed from the physical domain into a square computational domain. Then, all computations are based on the computational domain. Several examples are worked to demonstrate the convergence of the present DSC method. Excellent convergence behavior and accuracy, in comparison with exact results and or results obtained by other methods, are obtained. The effect of some geometric parameters on the frequency parameters of graphene sheet is investigated for skew and trapezoidal graphenes. Different combinations of boundary condition are also investigated. It can be also concluded that the classical plate theory can be suitable or an alternative approach for some special types of graphene. Also, the current transformation can be used for modeling of multilayer-graphene and other shaped graphene sheets with a quadrilateral domain.

Acknowledgements

The partial financial support of the Scientific and Technological Research Council of Turkey (Tübitak/112M879) is gratefully acknowledged. The authors would also like to thank Murat Gürses and Ali Kemal Baltacıoglu for their help during the computations.

References

1. Katsnelson, M.I., *Graphene: Carbon in Two Dimensions*, Cambridge University Press, UK (2012).
2. Hosseini Kordkheili, S.A. and Moshrefzadeh-Sani, H. "Mechanical properties of double-layered graphene sheets", *Comp. Mat. Sci.*, **69**, pp. 335-343 (2013).

3. Van Lier, G., Van Alsenoy, C. and Van Doren, V. "Ab initio study of the elastic properties of single-walled carbon nanotubes and graphene", *Chem. Phys. Lett.*, **326**, pp. 181-185 (2000).

4. Liu, Y., Xie, B., Zhang, Z., Zheng, Q. and Xu, Z. "Mechanical properties of graphene papers", *J. Mech. Phys. Solids*, **60**, pp. 591-605 (2012).

5. Novoselov, K.S., Geim, A.K., Morozov, S.V. and Jiang, D. "Two-dimensional gas of massless Dirac fermions in graphene", *Nature*, **438**, pp. 197-200 (2005).

6. Ohta, T., Bostwick, A., Seyller, T., Horn, K. and Rotenberg, E. "Controlling the electronic structure of bilayer graphene", *Science*, **313**, pp. 951-954 (2006).

7. Liew, K.M., Hu, Y.G. and He, X.Q. "Flexural wave propagation in single-walled carbon nanotubes", *J. Comp. Theor. Nanosci.*, **5**, pp. 581-586 (2008).

8. Liew, K.M., He, X.Q. and Kitipornchai, S. "Predicting nanovibration of multi-layered graphene sheets embedded in an elastic matrix", *Acta Mater.*, **54**, pp. 4229-4236 (2006).

9. Arash, B., Wang, Q. and Liew, K.M. "Wave propagation in graphene sheets with nonlocal elastic theory via finite element formulation", *Comp. Meth. Appl. Mech. Eng.*, **223**, pp. 1-9 (2012).

10. Mohammadi, M., Ghayour, M. and Farajpour, A. "Free transverse vibration analysis of circular and annular graphene sheets with various boundary conditions using the nonlocal continuum plate model", *Compos. Part B: Eng.*, **45**, pp. 32-42 (2013).

11. Mohammadi, M., Goodarzi, M., Ghayour, M. and Farajpour, A. "Influence of in-plane pre-load on the vibration frequency of circular graphene sheet via nonlocal continuum theory", *Compos. Part B: Eng.*, **51**, pp. 121-129 (2013).

12. Pouresmaeeli, S., Fazelzadeh, S.A. and Ghavanloo, E. "Exact solution for nonlocal vibration of double-orthotropic nanoplates embedded in elastic medium", *Compos. Part B: Eng.*, **43**, pp. 3384-3390 (2012).

13. Wang, Y.Z., Li, F.M. and Kishimoto, K. "Thermal effects on vibration properties of double-layered nanoplates at small scales", *Compos. Part B: Eng.*, **42**, pp. 311-317 (2011).

14. Zhang, C.-L. and Shen, H.-S. "Thermal buckling of initially compressed single-walled carbon nanotubes by molecular dynamics simulation", *Carbon*, **45**, pp. 2614-2620 (2007).

15. Shen, H.-S. and Zhang, C.-L. "Thermal buckling and postbuckling behavior of functionally graded carbon nanotube-reinforced composite plates", *Mater. Design*, **31**, pp. 3403-3411 (2010).

16. Shen, L., Shen, H.-S. and Zhang, C.-L. "Nonlocal plate model for nonlinear vibration of single layer graphene sheets in thermal environments", *Comp. Mater. Sci.*, **48**, pp. 680-685 (2010).

17. Lau, K.T., Chipara, M., Ling, H.Y. and Hui, D. "On the effective elastic moduli of carbon nanotubes for nano composite structures", *Compos. Part B: Eng.*, **35**, pp. 95-101 (2004).

18. Lau, K.T., Gu, C. and Hui, D. "A critical review on nanotube and nanotube/nanoclay related polymer composite materials", *Compos. Part B: Eng.*, **37**, pp. 425-436 (2006).

19. Civalek, Ö. and Demir, C. "Bending analysis of microtubules using nonlocal Euler-Bernoulli beam theory", *Appl. Math. Model.*, **35**, pp. 2053-2067 (2011).

20. Şimşek, M. "Vibration analysis of a single-walled carbon nanotube under action of a moving harmonic load based on nonlocal elasticity theory", *Physica E*, **43**, pp. 182-191 (2010).

21. Demir, C., Civalek, Ö. and Akgöz, B. "Free vibration analysis of carbon nanotubes based on shear deformable beam theory by discrete singular convolution technique", *Math. Comput. Appl.*, **15**, pp. 57-65 (2010).

22. Civalek, Ö., Demir, C. and Akgöz, B. "Free vibration and bending analyses of cantilever microtubules based on nonlocal continuum model", *Math. Comput. Appl.*, **15**, pp. 289-298 (2010).

23. Civalek, Ö. and Akgöz, B. "Free vibration analysis of microtubules as cytoskeleton components: Nonlocal Euler-Bernoulli beam modeling", *Sci. Iran. Trans. B*, **17**, pp. 367-375 (2010).

24. Akgöz, B. and Civalek, Ö. "Application of strain gradient elasticity theory for buckling analysis of protein microtubules", *Curr. Appl. Phys.*, **11**, pp. 1133-1138 (2011).

25. Akgöz, B. and Civalek, Ö. "Strain gradient elasticity and modified couple stress models for buckling analysis of axially loaded micro-scaled beams", *Int. J. Eng. Sci.*, **49**, pp. 1268-1280 (2011).

26. Akgöz, B. and Civalek, Ö. "A size-dependent shear deformation beam model based on the strain gradient elasticity theory", *Int. J. Eng. Sci.*, **70**, pp. 1-14 (2013).

27. Liew, K.M. and Han, J.B. "A four-note differential quadrature method for straight-sided quadrilateral Reissner/Mindlin plates", *Commun. Num. Meth. Eng.*, **13**, pp. 73-81 (1997).

28. Civalek, Ö. "Application of differential quadrature (DQ) and harmonic differential quadrature (HDQ) for buckling analysis of thin isotropic plates and elastic columns", *Eng. Struct.*, **26**, pp. 171-186 (2004).

29. Wei, G.W. "Discrete singular convolution for the solution of the Fokker-Planck equations", *J. Chem. Phys.*, **110**, pp. 8930-8942 (1999).

30. Wei, G.W. "Solving quantum eigenvalue problems by discrete singular convolution", *J. Phys. B At. Mol. Opti Phys.*, **33**, pp. 343-352 (2000).

31. Wei, G.W. "Discrete singular convolution for the Sine-Gordon equation", *Phys. D*, **137**, pp. 247-259 (2000).

32. Wei, G.W. "A unified approach for the solution of the Fokker-Planck equation", *J. Phys. A Math. Gen.*, **33**, pp. 4935-4953 (2000).

33. Wei, G.W. "Wavelets generated by using discrete singular convolution kernels", *J. Phys. B At. Mol. Opt. Phys.*, **33**, pp. 8577-8596 (2000).

34. Wei, G.W., Zhang, D.S., Althorpe, S.C., Kouri, D.J. and Hoffman, D.K. "Wavelet-distributed approximating functional method for solving the Navier-Stokes equation", *Comp. Phys. Commun.*, **115**, pp. 18-24 (1998).

35. Wei, G.W., Kouri, D.J. and Hoffman, D.K. "Wavelets and distributed approximating functionals", *Comp. Phys. Commun.*, **112**, pp. 1-6 (1998).

36. Zhao, Y.B., Wei, G.W. and Xiang, Y. "Discrete singular convolution for the prediction of high frequency vibration of plates", *Int. J. Solids Struct.*, **39**, pp. 65-88 (2002).

37. Zhao, Y.B., Wei, G.W. and Xiang, Y. "Plate vibration under irregular internal supports", *Int. J. Solids Struct.*, **39**, pp. 1361-1383 (2002).

38. Zhao, Y.B. and Wei, G.W. "DSC analysis of rectangular plates with non-uniform boundary conditions", *J. Sound Vib.*, **255**, pp. 203-228 (2002).

39. Hou, Y.G., Wei, G.W. and Xiang, Y. "DSC-Ritz method for the free vibration analysis of Mindlin plates", *Int. J. Num. Meth. Eng.*, **62**, pp. 262-288 (2005).

40. Zhao, S. and Wei, G.W. "Comparison of the discrete singular convolution and three other numerical schemes for solving Fisher's equation", *SIAM J. Sci. Comp.*, **25**, pp. 127-147 (2003).

41. Wei, G.W. and Yun, G. "Conjugate filter approach for solving Burgers' equation", *J. Comp. Appl. Math.*, **149**, pp. 439-456 (2002).

42. Wei, G.W. "A new algorithm for solving some mechanical problems", *Comput. Meth. Appl. Mech. Eng.*, **190**, pp. 2017-2030 (2001).

43. Wei, G.W. "Vibration analysis by discrete singular convolution", *J. Sound Vib.*, **244**, pp. 535-553 (2001).

44. Wei, G.W. "Discrete singular convolution for beam analysis", *Eng. Struct.*, **23**, pp. 1045-1053 (2001).

45. Wei, G.W., Zhao, Y.B. and Xiang, Y. "Discrete singular convolution and its application to the analysis of plates with internal supports. Part 1: Theory and algorithm", *Int. J. Num. Meth. Eng.*, **55**, pp. 913-946 (2002).

46. Wei, G.W., Zhao, Y.B. and Xiang, Y. "A novel approach for the analysis of high-frequency vibrations", *J. Sound Vib.*, **257**, pp. 207-246 (2002).

47. Wei, G.W., Zhao, Y.B. and Xiang, Y. "The determination of natural frequencies of rectangular plates with mixed boundary conditions by discrete singular convolution", *Int. J. Mech. Sci.*, **43**, pp. 1731-1746 (2001).

48. Xiang, Y., Zhao, Y.B. and Wei, G.W. "Discrete singular convolution and its application to the analysis of plates with internal supports. Part 2: Applications", *Int. J. Num. Meth. Eng.*, **55**, pp. 947-971 (2002).

49. Wan, D.C. and Wei, G.W. "Numerical solutions of incompressible Euler and Navier-Stokes equations by efficient discrete singular convolution method", *Acta Mech. Sinica*, **16**, pp. 223-239 (2000).

50. Seçkin, A. and Sarıgül, A.S. "Free vibration analysis of symmetrically laminated thin composite plates by using discrete singular convolution (DSC) approach: Algorithm and verification", *J. Sound Vib.*, **315**, pp. 197-211 (2009).

51. Civalek, Ö. "An efficient method for free vibration analysis of rotating truncated conical shells", *Int. J. Pres. Ves. Pip.*, **83**, pp. 1-12 (2006).

52. Civalek, Ö. "Three-dimensional vibration, buckling and bending analyses of thick rectangular plates based on discrete singular convolution method", *Int. J. Mech. Sci.*, **49**, pp. 752-765 (2007).

53. Civalek, Ö. "Free vibration analysis of composite conical shells using the discrete singular convolution algorithm", *Steel Compos. Struct.*, **6**, pp. 353-366 (2006).

54. Civalek, Ö. "Linear vibration analysis of isotropic conical shells by discrete singular convolution (DSC)", *Struct. Eng. Mech.*, **25**, pp. 127-130 (2007).

55. Civalek, Ö. "A parametric study of the free vibration analysis of rotating laminated cylindrical shells using the method of discrete singular convolution", *Thin Wall. Struct.*, **45**, pp. 692-698 (2007).

56. Civalek, Ö. "Free vibration and buckling analyses of composite plates with straight-sided quadrilateral domain based on DSC approach", *Finite Elem. Anal. Des.*, **43**, pp. 1013-1022 (2007).

57. Civalek, Ö. "A four-node discrete singular convolution for geometric transformation and its application to numerical solution of vibration problem of arbitrary straight-sided quadrilateral plates", *Appl. Math. Model.*, **33**, pp. 300-314 (2009).

58. Ansari, A., Sahmani, S. and Arash, B. "Nonlocal plate model for free vibrations of single-layered graphene sheets", *Phys. Lett. A*, **375**, pp. 53-62 (2010).

59. Babaei, H. and Shahidi, A.R. "Vibration of quadrilateral embedded multilayered graphene sheets based on nonlocal continuum models using the Galerkin method", *Acta Mech. Sin.*, **27**, pp. 967-976 (2011).

60. Alibeygi Beni, A. and Malekzadeh, P. "Nonlocal free vibration of orthotropic non-prismatic skew nanoplates", *Compos. Struct.*, **94**, pp. 3215-3222 (2012).

Biographies

Bekir Akgöz is currently a PhD degree student in Civil Engineering at Akdeniz University, Turkey. He has over 25 published journal papers (about 20 in SCI&SCI-Expanded Journals) and several conference proceedings. His research interests include mathematical modeling of micro- and nanostructures, higher-order continuum theories, functionally graded materials, beam and plate theories.

Ömer Civalek holds two PhD degrees in Structural and Mechanical Engineering from Dokuz Eylül University, Turkey (Structural Engineering), and the University of Firat, Turkey (Applied Mechanics), respectively, and is currently Professor in the Faculty of Engineering at the University of Akdeniz, Turkey. He has authored over 150 refereed journal papers (about 90 in SCI&SCI-Expanded Journals), and over 20 papers presented at various conferences. His research emphasis has been on solid mechanics, vibration (especially plates and shells), computational mechanics, laminated structures, structural dynamics, modeling of nanostructures, and artificial neural networks applied to applied mechanics problems.